tions involving certain kinds of tree ring data. Changing atmospheric CO_2 could introduce nonclimatic growth fluctuations that could interfere with calibration of climate and its reconstruction. Techniques like those now applied to remove biological age trends or effects of ecological factors (*27*) would have to be developed to separate such effects from the climate signal in tree ring data. Conversely, the climatic and ecological information in tree rings could be applied to isolate and enhance the apparent CO_2 signal. Such enhanced proxy records of atmospheric CO_2 might be developed at different localities from the beginning of the industrial era.

It will be necessary to determine the geographic extent of the postulated fertilization effect and to test high-altitude growth trends against longer and geographically more representative sets of climatic data. In addition, the effects of changing CO_2 concentrations on productivity, growth, and development of conifers growing under high-altitude conditions should be determined experimentally.

VALMORE C. LAMARCHE, JR.
DONALD A. GRAYBILL
HAROLD C. FRITTS
MARTIN R. ROSE
Laboratory of Tree-Ring Research,
University of Arizona, Tucson 85721

References and Notes

1. W. C. Clark, Ed., *Carbon Dioxide Review: 1982* (Oxford Univ. Press, New York, 1982).
2. Carbon Dioxide Assessment Committee, *Changing Climate* (National Academy Press, Washington, D.C., 1983).
3. G. M. Woodwell *et al.*, *Science* **222**, 1081 (1983).
4. S. Seidel and D. Keyes, *Can We Delay a Greenhouse Warming*? (Environmental Protection Agency, Washington, D.C., 1983).
5. E. R. Lemon, Ed., *CO_2 and Plants: The Response of Plants to Rising Levels of Atmospheric Carbon Dioxide* (Westview, Boulder, Colo., 1983).
6. H. H. Rogers, J. F. Thomas, G. E. Bingham, *Science* **220**, 428 (1983); K. Green and R. Wright, *Ecology* **58**, 687 (1977).
7. As discussed by L. Machta (*2*, pp. 242–251), the increasing amplitude of the annual cycle of atmospheric CO_2 implies that terrestrial vegetation may be increasingly active in response to increasing average CO_2 concentrations. Stable carbon isotopic data [S. W. Leavitt and A. Long, *Tellus* **358**, 92 (1983)] suggest that the biosphere has acted as a net sink for CO_2 since about 1965; if so, increased productivity in natural vegetation stimulated by increasing CO_2 could be a contributing factor.
8. V. C. LaMarche, Jr., and C. W. Stockton, *Tree-Ring Bull.* **44**, 21 (1974).
9. V. C. LaMarche, Jr., *Science* **183**, 1043 (1974).
10. D.A.G. and M.R.R. collected tree ring samples at 3325 m on Mount Jefferson, Toquima Range, Nevada, on 11 August 1981.
11. D.A.G. and M.R.R. collected samples from 13 trees at Campito Mountain (3400 m) and from 15 trees at Sheep Mountain (3500 m) on 31 October 1983.
12. Crooked Creek Station (3094 m) was established in 1948 and discontinued in 1977; Barcroft Station (3801 m) was established in 1953 and discontinued in 1981. Early observations are summarized by N. Pace, D. W. Kiepert, and E. M. Nissen [*Climatological Data Summary for the Crooked Creek Laboratory, 1949–1967, and the Barcroft Laboratory, 1953–1967* (White Mountain Research Station, University of California, Berkeley, 1968)]. Instrument relocation in 1954 may have affected minimum temperatures at the lower station [V. C. LaMarche, Jr., *Quat. Res. (N.Y.)* **3**, 632 (1973)]. From 1955 on, data for these stations were published in *Climatological Data: California* (U.S. Weather Bureau and National Oceanographic and Atmospheric Administration, Washington, D.C.).
13. L. G. Drew, Ed., *Tree-Ring Chronologies of Western America: California and Nevada* (Laboratory of Tree-Ring Research, University of Arizona, Tucson, 1972).
14. Recent growth rate data are presented as simple average ring widths (i) to avoid creating any artificial trends in the critical recent decades which could possibly be introduced by the standardization process normally used to transform ring widths to dimensionless growth indices and (ii) in order that absolute growth rate changes could be calculated. Published indices are presented in original form only to provide basic documentation of growth fluctuations before the beginning of the postulated CO_2 effect. The disparity in units does not affect the comparison of long-term trends in the two sets of data.
15. R. S. Bradley, R. G. Barry, G. Kiladis, *Climatic Fluctuations of the Western United States During the Period of Instrumental Records* (Contribution No. 42, Department of Geology and Geography, University of Massachusetts, Amherst, 1982). Data are statewide monthly averages from the late 19th century to 1970 and include Colorado, New Mexico, Utah, Nevada, and California.
16. W. Bischof, *Tellus* **14**, (1962); C. D. Keeling, *ibid.* **12**, 200 (1960); C. D. Keeling, R. B. Bacastow, T. P. Whorf, in (*1*), p. 377.
17. Geophysics Research Directorate, *Handbook of Geophysics* (Macmillan, New York, 1960).
18. Environmental Science Services Administration, *U.S. Standard Atmosphere Supplements, 1966* (Government Printing Office, Washington, D.C., 1966).
19. W. Tranquillini, *Physiological Ecology of the Alpine Timberline* (Springer-Verlag, New York, 1979).
20. J. Gale, *Ecology* **53**, 494 (1972); *Ecol. Conserv.* **5**, 289 (1973).
21. H. A. Mooney, R. D. Wright, B. R. Strain, *Am. Midl. Nat.* **72**, 281 (1964); H. A. Mooney, B. R. Strain, M. West, *Ecology* **47**, 490 (1966).
22. W. Koch, *Flora* **B158**, 402 (1969).
23. This is a consensus value reported by R. Kerr [*Science* **222**, 1107 (1983)]; the range cited is from about 270 ppm (ice core data) to 260 to 276 ppm (tree ring isotope results).
24. This is based on the 1980 Mauna Loa value of 238 ppm given by C. D. Keeling, R. B. Bacastow, and T. P. Whorf [in (*1*), p. 377], adjusted for an annual increase of about 1 ppm.
25. D. N. Baker and H. Z. Henoch, in (*5*), pp. 107–130.
26. A further possibility is that there are other morphological, physiological, or metabolic effects of elevated CO_2 that in some way preferentially enhance growth in plants limited to subalpine or other cold habitats and that these effects are operating in addition to the postulated direct fertilization effect.
27. D. A. Graybill, in *Climate from Tree Rings*, M. K. Hughes, P. M. Kelly, J. R. Pilcher, and V. C. LaMarche, Jr., Eds. (Cambridge Univ. Press, Cambridge, 1982), pp. 21–28; G. R. Lofgren and J. H. Hunt, *ibid.*, pp. 50–56.
28. We thank M. McCarthy for aid in sampling, F. Telewski for helpful discussions, M. Harrington and A. Allen for manuscript preparation, and the National Science Foundation for partial support under grant EAR 8018687.

8 March 1984; accepted 28 June 1984

Periodic Interfacial Precipitation in Polymer Films

Abstract. *Interfacial precipitation of silver halides in water-swollen polymer films occurred in complex, multilayered patterns if the concentrations of counterdiffusing reactants were unequal or decreased at different rates. Development of the rapidly forming Liesegang rings, which extend the phenomenon of periodic precipitation to the submicrometer range, is attributable to the combined effect of a moving reaction zone and periodic immobilization of colloidal silver halide.*

When solutions of electrolytes in which all convection has been eliminated—for example, $0.01M$ $Pb(NO_3)_2$ and $0.1M$ NaI in 1 percent agar or gelatin gels—are placed side by side in a test tube or petri dish, PbI_2 precipitates on interdiffusion of Pb^{2+} and I^- in the form of separate layers that are parallel to the diffusion front and 0.01 mm to several millimeters thick. This periodic precipitation, known as the Liesegang phenomenon (*1*), has been investigated intensively (*2*–*4*). During research on interfacial reactions in polymer films (*5*), I was able to produce a similar effect in a much denser matrix, down to 0.1 μm in thickness and with excellent resolution, when silver and halide ions were allowed to diffuse against each other in a water-swollen polyvinyl alcohol (PVA) film.

Two types of experiments were carried out. In the first, heat-sealed pouches of commercial PVA film (thickness, 0.11 mm when dry and 0.18 mm when wet; water content, 57 percent) were filled with silver nitrate solution and immersed in much larger volumes of equimolar sodium halide solutions. Because of their unequal volumes, both solutions were self-diluting at different rates during the reaction, and the ion concentration difference $D = [X^-] - [Ag^+]$ and the ion concentration ratio $R = [X^-]/[Ag^+]$ changed at a rate dependent on the volume difference. In the second type of experiment, water-swollen PVA film was used to separate equal volumes of anion and cation solutions in a diffusion cell. This allowed D and R to be kept constant or to be changed at any rate desired by diluting one compartment.

Precipitation began to show in the films within seconds. Reactions were terminated by emptying the pouches or cells and rinsing the films in distilled water for 1 hour. The films were then dried at 50°C in a vacuum. Cross sections were viewed through a microscope in both the dry and water-swollen states.

In the pouch-forming PVA films all silver halides precipitated in a complex, multilayered pattern (Fig. 1). Usually a strong, primary band of precipitate formed first, closer to the surface contacting the halide solution but separated from it by a precipitate-free zone. Extending from this primary band of precipitate toward the inner pouch surface in contact with the self-diluting $\mathrm{AgNO_3}$ solution were other, much thinner, very sharply defined layers. Often what appeared to be one layer of precipitate was at higher magnification segregated into even thinner multiple layers. I sometimes observed the regular spacing characteristic of Liesegang rings (Fig. 1a) and, especially after long reaction times, zones of grainy precipitate, possibly the result of secondary crystal growth (*6*). The layered but not the grainy precipitate often produced strong birefringence in polarized light (Fig 1, b and c). If the placement of reactants was reversed—that is, if $\mathrm{AgNO_3}$ was used in excess volume outside the pouch and NaI inside—the location of the primary precipitate remained unchanged, but the secondary, finer layers were now squeezed into the more narrow zone in contact with the self-diluting NaI solution. The number of layers and the total space occupied by them was largest for the smallest pouches, which, as confirmed by silver analysis, were self-diluting at the highest rate and therefore produced the greatest change in D and R.

With the diffusion cell, D and R could be kept nearly constant throughout the reaction. Only at very short reaction times (<1 minute) were several thin layers visible in a zone that was wider at lower concentrations and larger R (Fig. 2, d to f). I assume that this zone is located in that part of the film's cross section where anion and cation fluxes are equivalent and that its width is determined by the slope of concentration gradients; in thick films or at low concentrations greater ion overlap occurs before the solubility product is reached, resulting in a wide reaction zone in which a fine structure can easily be seen (Fig. 2f), whereas the opposite conditions give narrow reaction zones and poor resolution (Fig. 2d). In addition, any imbalance in ion concentration ($R > 1$) leads to a corresponding slow movement of the reaction front toward the side of lower concentration and a further spreading of the bands. A fine structure of extremely close lines could be seen, but only after short reaction times, even when D was zero ($R = 1$), which makes it likely that only a concentration gradient, not a shift of the reaction zone, is necessary for periodically banded precipitation (*7*).

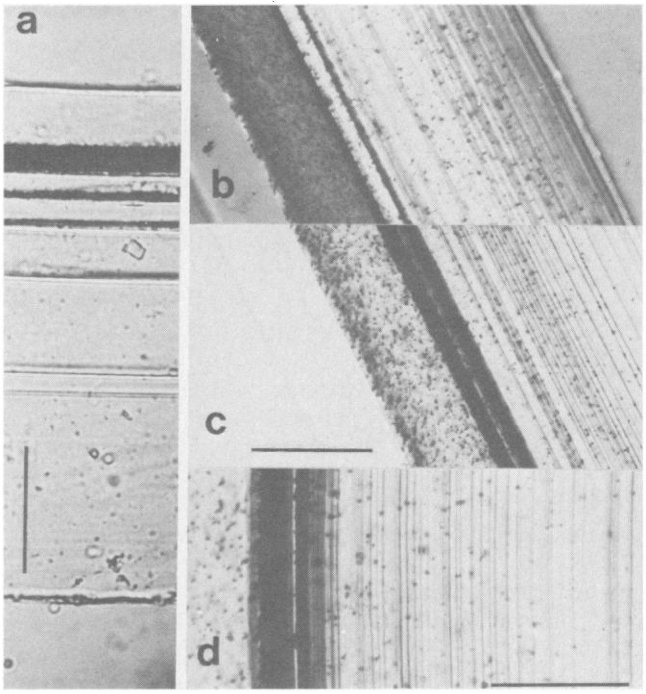

Fig. 1. Photomicrographs of silver halide precipitated in water-swollen PVA film. Ten-milliliter pouches with $\mathrm{AgNO_3}$ solution were immersed in 100 ml of sodium halide solution. (a) AgI from $0.1M$ $\mathrm{AgNO_3}$ + $0.1M$ NaI after 20 minutes; NaI-contacting side is up. Scale bar, 0.05 mm. (b and c) AgBr from $0.05M$ $\mathrm{AgNO_3}$ + $0.05M$ NaBr after 16 hours; in polarized light with crossed (b) and uncrossed (c) polarizers. Scale bar, 0.05 mm. (d) Same sample at higher magnification; NaBr-contacting side is at left. Scale bar, 0.025 mm.

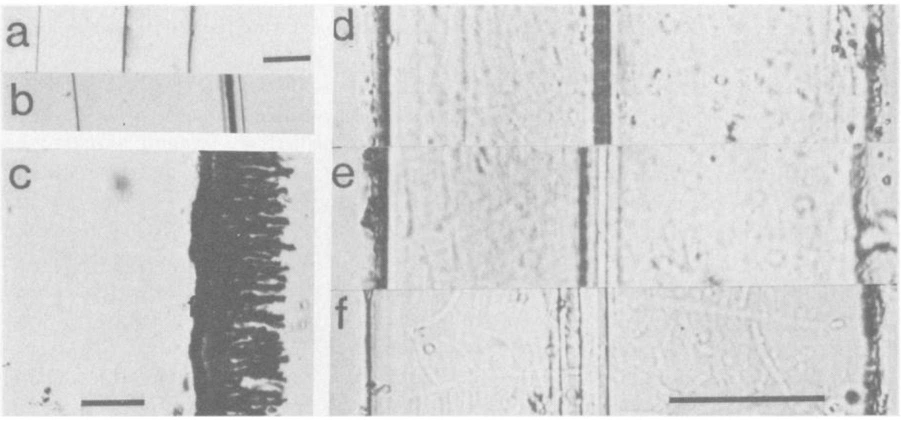

Fig. 2. Photomicrographs of silver halide in water-swollen PVA films, diffusion cell arrangement. (a) AgI from $0.1M$ $\mathrm{AgNO_3}$ + $0.1M$ NaI after 25 seconds. Scale bar, 0.05 mm. (b) AgI from $0.1M$ $\mathrm{AgNO_3}$ + 0.025 NaI after 5 minutes. Scale bar, 0.05 mm. (c) Mixed AgI/AgCl precipitate from $0.05M$ $\mathrm{AgNO_3}$ and $0.025M$ NaI + $0.025M$ NaCl after 20 minutes. Borders of film are not visible; $\mathrm{AgNO_3}$-contacting sides are at left. Scale bar, 0.02 mm. (d to f) AgI, after 45 seconds, from (d) $0.1M$ $\mathrm{AgNO_3}$ + $0.125M$ NaI ($D = 0.025$, $R = 1.25$); (e) $0.05M$ $\mathrm{AgNO_3}$ + $0.075M$ NaI ($D = 0.025$; $R = 1.5$); and (f) $0.025M$ $\mathrm{AgNO_3}$ + $0.05M$ NaI ($D = 0.025$, $R = 2.0$). The $\mathrm{AgNO_3}$-contacting side is at left. Scale bar, 0.05 mm.

After longer reaction times (>2 minutes), all fine structure became submerged in the increasingly dense precipitate. Then only one, rarely two, narrow layers, whose locations were dependent on D and R, were visible closer to the side of the lower ion concentrations (Fig. 2, a and b). Sometimes dendrites grew toward the side contacting the halide solution (Fig. 2c). If D was too large, precipitation occurred outside the film in the more dilute solution. Silver analysis showed that ion diffusion was the rate-determining step for precipitation (*8*).

The effect of changes in D on the spacing of precipitate zones and on the fine structure within them is shown in Fig. 3, a and b. Simulating the pouch system by continuous dilution of the $\mathrm{AgNO_3}$ solution gave a discontinuous system of thin and parallel layers, as obtained with the pouches (Fig. 3c).

In the model of a matrix-supported interfacial precipitation, in which the influx of reactants equals their removal, the width of the reaction zone, or of ion overlap, should depend on the relative rates of diffusion on the one hand and the rates of reaction or solubility of the precipitate on the other. Indeed, the precipitates with the lower solubility, AgI, AgBr, and $\mathrm{Mg_3(PO_4)_2}$, formed sharper layers than AgCl. The even more soluble salt $\mathrm{Ag_2Cr_2O_7}$ showed the biggest grain size and the most diffuse precipitate boundaries, that is, the greatest region of ion concentration overlap (Fig. 4, a and b) (*9*).

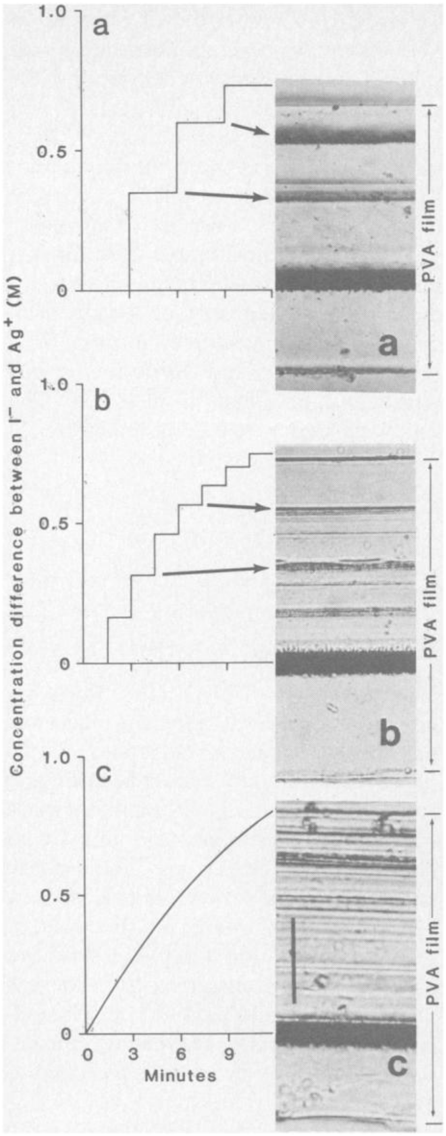

Fig. 3. Precipitate of AgI in water-swollen PVA film after stepwise dilution (a and b) and continuous dilution (c) of $AgNO_3$ solution. Initially, 0.1*M* $AgNO_3$ and 0.1*M* NaI (60 cm^2 each) were present on two sides of the diffusion cell, separated by PVA film 40 mm in diameter. The $AgNO_3$ was diluted (a) every 3 minutes to 65 percent of the previous value, (b) every 1.5 minutes to 81 percent of the previous value, or (c) continuously. The $AgNO_3$-contacting side is up. Scale bar, 0.05 mm. Arrows in (a) and (b) point to lines formed at equal *D*. Note the fine structure in (b).

In appearance and mode of formation these thin layers resemble Liesegang rings in miniature, and a similar mechanism of postnucleation colloid focusing (*7, 10, 11*) can be assumed, aided by shifts in the reaction zone: freshly formed, very finely dispersed and charged silver halide colloid is continuously transported through the PVA film cross section, remaining focused in the gradually shifting reaction zone, which is also the zone of lowest ionic strength and greatest colloid stability. At certain intervals after the colloid has reached a critical size by autocatalytic growth or reached a critical charge density, immobilization occurs and the process repeats itself. The reaction front can move either slowly because of an ion concentration imbalance ($D/dt = 0; R > 1$) (Fig. 2, d to f) or quickly in response to an imposed dilution scheme ($D/dt > 0$) (Figs. 1 and 3c), providing in both cases a more or less expanded view of periodic precipitation.

A variety of regular precipitation patterns can arise as the combined effects of the moving reaction zone and periodic precipitation, including evenly spaced layers when the dilution of one ion solution results in a constant rate of change of *D* and "revertly" spaced (progressively closer) layers (*3, 11*) if *D* changes at decreasing rates (Fig. 3) and precipitation occurs at regular time intervals. If precipitation occurs at progressively longer intervals, Liesegang rings with progressively wider spacing are formed because the concentration of charged colloid is so low that it travels farther and farther before reaching the critical size and concentration at which it becomes immobilized (Fig. 1a). Figure 4c shows a series of revertly spaced AgCl layers splitting off from primary layers in a manner suggesting the sweeping and focusing action of an electrophoretic process.

Polyvinyl alcohol film, a much denser matrix than is commonly used for Liesegang experiments, probably allows much finer spacing of periodic precipitation because of reduced diffusion rates and mobility of ions, colloid, and molecular silver halide. A denser matrix may also allow the colloid to grow to a larger size before it becomes unstable and forms a crystalline precipitate. By extrapolation, one would expect even closer spacings and narrower lines to form in denser, less permeable materials.

Besides providing a tool for the modification and study of polymer membranes and precipitation processes, these experiments show that the phenomenon of periodic precipitation extends to materials that in scale and physical nature resemble biological membranes. The observed structures may be characteristic of all systems over a wide range of dimensions and densities wherever a fast reaction is fed by a slow, unidirectional diffusion of reactants and formation of a crystalline, insoluble precipitate is preceded by a charged colloidal phase that can be transported by an ionic field. A reaction-diffusion theory has been used to explain banded patterns in metamorphic rocks (*12*). In molten rock a precipitation front can also propagate through conductive cooling, reducing the solubility of dissolved minerals; with the cold front acting in place of a diffusing reactant, banded structures can presumably arise by the same combination of a moving reaction zone and periodic immobilization.

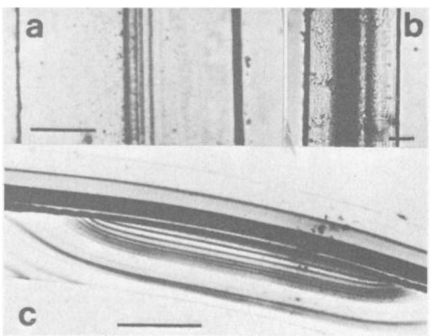

Fig. 4. Photomicrographs of precipitates in PVA film (pouch system). (a) $(Mg)_3(PO_4)_2$ from 0.3*M* $MgCl_2$ (inside) + 0.2*M* Na_3PO_4 after 16 hours; (b) $Ag_2Cr_2O_7$ from 0.1*M* $AgNO_3$ (inside) + 0.05*M* $K_2Cr_2O_7$ after 5 minutes; Mg^{2+}- and Ag^+-contacting sides are at right. Scale bars, 0.05 mm; (c) AgCl from 0.1*M* $AgNO_3$ + 0.1*M* NaCl after 20 minutes, showing nascent secondary lines with revert spacing. Careful examination reveals a wave-like distortion of the primary band on points of secondary line origins. The Ag^+-contacting side is down. Scale bar, 0.1 mm.

KARL F. MUELLER

Central Research,
CIBA-GEIGY Corporation,
Ardsley, New York 10502

References and Notes

1. R. E. Liesegang, *Naturwiss. Wochenschr.* **11**, 353 (1896).
2. F. E. Lloyd and V. Morawek, *J. Phys. Chem.* **35**, 1512 (1931); E. S. Hedges, *Liesegang Rings and Other Periodic Structures* (Chapman & Hall, London, 1932).
3. S. C. Müller, S. Kai, J. Ross, *J. Phys. Chem.* **86**, 4078 (1982); *ibid.* **87**, 806 (1983); *Science* **216**, 635 (1982).
4. N. Kanniah, F. D. Guanam, P. Ramasamy, *J. Colloid Interface Sci.* **94**, 412 (1983).
5. K. F. Mueller and S. J. Heiber, *J. Appl. Polym. Sci.* **27**, 4043 (1982); U.S. Patent 4,423,099.
6. S. C. Müller, S. Kai, J. Ross, *J. Phys. Chem.* **86**, 4294 (1982).
7. G. Venzl and J. Ross, *J. Chem. Phys.* **77**, 1302 (1982).
8. At equimolar silver and iodide concentrations between 0.025 and 0.1*M*, the reaction in 0.11 mm of PVA was first order with respect to Ag^+, with a reaction constant of $6.9 \pm 0.2 \times 10^{-5}$ mol/cm^2-min, at least up to 5 minutes' reaction time.
9. The solubility products of the precipitates at 25°C are (moles per liter): AgI (1.5×10^{-16}), AgBr (7.7×10^{-13}), AgCl (1.56×10^{-10}), $Ag_2Cr_2O_7$ (2.0×10^{-7}) [R. C. Weast, Ed., *Handbook of Chemistry and Physics* (CRC Press, Boca Raton, Fla., ed. 54, 1973), p. B-232], and $Mg_3(PO_4)_2 \cdot 8H_2O$ (6.3×10^{-26}) [A. W. Taylor, A. W. Frazier, E. L. Gurney, J. P. Smith, *Trans. Faraday Soc.* **59**, 1585 (1963)].
10. D. Feinn, P. Ortoleva, W. Scalf, S. Schmidt, M. Wolff, *J. Chem. Phys.* **69**, 29 (1978); S. Kai, S. C. Müller, J. Ross, *ibid.* **76**, 1392 (1982); R. Lovett, P. Ortoleva, J. Ross, *ibid.* **69**, 947 (1978).
11. M. Flicker and J. Ross, *ibid.* **60**, 3458 (1974).
12. P. Ortaleva, E. Merino, P. Strickholm, *Am J. Sci.* **282**, 617 (1982).

30 January 1984; accepted 9 May 1984